Sampling Phasic Dopamine Signaling with Fast-Scan Cyclic Voltammetry in Awake, Behaving Rats

S.M. Fortin,[1] J.J. Cone,[1] S. Ng-Evans,[2] J.E. McCutcheon,[3] and M.F. Roitman[1,4]

[1]Graduate Program in Neuroscience, University of Illinois at Chicago, Chicago, Illinois
[2]Department of Psychiatry and Behavioral Sciences, University of Washington, Seattle, Washington
[3]Department of Cell Physiology & Pharmacology, University of Leicester, Leicester, United Kingdom
[4]Department of Psychology, University of Illinois at Chicago, Chicago, Illinois

Fast-scan cyclic voltammetry (FSCV) is an electrochemical technique that permits the in vivo measurement of extracellular fluctuations in multiple chemical species. The technique is frequently utilized to sample sub-second (phasic) concentration changes of the neurotransmitter dopamine in awake and behaving rats. Phasic dopamine signaling is implicated in reinforcement, goal-directed behavior, and locomotion, and FSCV has been used to investigate how rapid changes in striatal dopamine concentration contribute to these and other behaviors. This unit describes the instrumentation and construction, implantation, and use of components required to sample and analyze dopamine concentration changes in awake rats with FSCV. © 2015 by John Wiley & Sons, Inc.

Keywords: fast-scan cyclic voltammetry • dopamine • reward • nucleus accumbens • motivation • reinforcement

How to cite this article:
Fortin, S.M., Cone, J.J., Ng-Evans, S., McCutcheon, J.E., and Roitman, M.F. 2015. Sampling Phasic Dopamine Signaling with Fast-Scan Cyclic Voltammetry in Awake, Behaving Rats. *Curr. Protoc. Neurosci.* 70:7.25.1-7.25.20.
doi: 10.1002/0471142301.ns0725s70

BASIC PROTOCOL

The neurotransmitter dopamine plays a central role in the underlying mechanisms governing motivation, reinforcement, and motor behavior, while its pathology is associated with neurological disorders including schizophrenia and Parkinson's disease. Multiple approaches have been utilized to understand dopamine's function in these processes. Here, we focus on an analytical tool, fast-scan cyclic voltammetry (FSCV), to measure dopamine concentration in dopamine terminal regions of behaving animals. FSCV measures dopamine concentration in situ and with spatial (micrometer) and temporal (subsecond) resolution that is unparalleled by alternative in vivo techniques used to measure neurochemical transmission such as microdialysis and positron emission tomography (PET; Sossi and Ruth, 2005; Watson et al., 2006).

The spatial and temporal acuity together with the high chemical sensitivity (nanomolar range) of FSCV make it particularly well suited for quantification of burst-like (phasic) dopamine release events that are critical for learning (Stuber et al., 2008; Flagel et al., 2011; Schultz, 2013) and goal-directed behavior (Phillips et al., 2003b; Roitman et al., 2004). While the techniques described here are optimized for correlating phasic dopamine release in the nucleus accumbens (NAc) with rat behavior, FSCV can also

Current Protocols in Neuroscience 7.25.1-7.25.20, January 2015
Published online January 2015 in Wiley Online Library (wileyonlinelibrary.com).
doi: 10.1002/0471142301.ns0725s70

detect extracellular concentration changes of other analytes including serotonin (Hashemi et al., 2009, 2011), norepinephrine (Baur et al., 1988; Park et al., 2011), adenosine (Swamy and Venton, 2007), oxygen (Venton et al., 2003), histamine (Hashemi et al., 2011), nitric oxide (Iravani et al., 1998), ascorbic acid (Venton et al., 2002), and pH (Runnels et al., 1999). Excellent review papers are available that thoroughly describe how the approach has been used in awake and behaving rats (Stamford, 1990; Phillips et al., 2003a; Robinson et al., 2003). The technique has also been used in other species including Drosophila (Vickrey et al., 2009), lamprey (Ryczko et al., 2013), mice (Natori et al., 2009; Parker et al., 2010; Ehrich et al., 2014), monkeys (Ariansen et al., 2012; Schluter et al., 2014), and humans (Kishida et al., 2011).

Importantly, FSCV permits correlating dopamine fluctuations with an animal's behavior, a feature that has greatly advanced our understanding of the regulation of dopamine signaling (Garris et al., 1997, 1999; Venton et al., 2006; Owesson-White et al., 2012) and its role in learning (Owesson-White et al., 2008; Stuber et al., 2008; Aragona et al., 2009), goal directed behavior (Garris et al., 1999; Phillips et al., 2003b; Roitman et al., 2004; Cheer et al., 2007), and decision-making (Day et al., 2010; Sugam et al., 2012). The reader is strongly encouraged to review the published works of Dr. R. Mark Wightman and his collaborators from 1995 to the present for use of the technique in behaving subjects (Stamford et al., 1984; Kuhr and Wightman, 1986; Wightman et al., 1988; Jones et al., 1996; Garris et al., 1997; Venton et al., 2002; Phillips et al., 2003a; Heien et al., 2004; Keithley et al., 2011). Here, we focus on the use of carbon fiber microelectrodes that are driven acutely (once per recording session) through the brain of awake, behaving rats to dopamine terminal regions. Recent work from the laboratory of Dr. Paul Phillips has established a different approach that utilizes a chronic indwelling electrode (Clark et al., 2010), and the reader is also encouraged to review work from this group.

Strategic Planning

FSCV is best suited for capturing fast, phasic *changes* in dopamine concentration because background subtraction must occur temporally close (within ~10 to 90 sec) to the release event. Therefore, changes in dopamine concentration over the course of minutes to hours are better studied via a non-differential technique such as microdialysis. In awake and behaving animals, FSCV recordings are most easily obtained soon after the animal recovers (within 5 to 10 days) from implantation of a cannula, reference, and stimulating electrode (see below for detail). For this reason, experimental design timelines should be carefully planned, especially for behavioral experiments, which require animal training. If possible, animals should be trained to a behavioral criterion before surgical implantation of the cannula, and given retraining sessions following recovery. Experimental designs that incorporate a within-session experimental manipulation are ideally suited for FSCV (see, e.g., Cone et al., 2014), while experiments that require comparisons within-animal but across days present complications. Each placement of the electrode samples from a different set of dopamine release sites (Venton et al., 2003; Dreyer et al., 2010), and thus differences in magnitude of dopamine release across recording locations become difficult to interpret. We acknowledge that in cases where a within-subjects factor cannot be adequately integrated into the experimental design, obtaining data from a large number of animals in the different conditions will make between-subjects comparisons more robust.

Fast-Scan Cyclic Voltammetry (FSCV) is a powerful technique that allows dopamine concentration to be measured in awake, behaving subjects with high temporal and spatial acuity. The most critical factor in conducting these experiments is fabrication and assessment of the carbon-fiber recording electrodes, as measurements are heavily dependent

on electrode quality. In addition, a proper understanding of the analysis conventions, particularly interpretation of color plot data, is a vital aspect that will aid with performing experiments, interpreting data, and troubleshooting.

Materials

Isopropyl alcohol (Sigma-Aldrich, cat. no. I9030), filtered
Devcon 5-min epoxy (Fisher Scientific, cat. no. NC9987160)
1 N HCl (Fisher Scientific, cat. no. SA48-1)
Sprague Dawley Rats (Charles River)
Ketamine
Xylazine
Betadine
Ethanol
Jet-repair dental acrylic (Lang Dental, cat. no. 1405)

Carbon fiber (7 μm in diameter; Goodfellow Corp., cat. no. C005722)
10-cm borosilicate glass capillary tube (4 in., 0.6 mm OD × 0.4 mm ID; A-M Systems, cat. no. 624500)
Thermo/Barnant vacuum pump (Midland Scientific, cat. no. BAR 400-3910)
Vertical microelectrode puller (Narishige Group, cat. no. PE-22)
Scissors
Scalpel with a #11 surgical blade (Fisher Scientific, cat. no. 14-840-16)
Light microscope with a graticule in the eyepiece
Microscope slide coated in clear packing tape
Sculpting putty
Gold pins (Newark, cat. no. SPC15509)
Bare wires (30-G, 3 in. (7.6 cm), UL1423 type, Squires Electronics, Cornelius, or custom)
Silverprint conductive paint (GC Electronics, cat. no. 22-024)
Three types of heat-shrinkable flexible polyolefin tubing: 3/32 in. i.d. (APD, cat. no. 00-051128-59888-7), 3/64 in. i.d., clear (Digi-Key, cat. no. KY364C-ND), and 3/64 in. i.d. (Altex, cat. no. HST3/64)
Micromanipulator (University of Illinois at Chicago Research Resources Center, custom; Fig. 7.25.3A), loaded with a carbon fiber electrode (Fig. 7.25.3).
Silver wire (0.5 mm diameter, Sigma-Aldrich, cat. no. 327026-20 G)
9 V battery with stainless steel or copper wires soldered to the terminals
Twisted stainless-steel stimulating electrodes (20 mm, Plastics One, cat. no. MS303T/2-B/SPC)
Animal clippers
Small animal stereotaxic instrument (David Kopf Instruments, model 900) with:

- Non-rupture ear bars (David Kopf Instruments, cat. no. 955)
- Clamp rod for stereotaxic frame (BASi, cat. no. MD-1521)
- Probe clamp (BASi, cat. no. MD-1520)

Gauze
Stainless steel surgical screws (3/16 in., Small Parts through Amazon, ASIN, cat. no. B000FN5XE0)
Surgical drill bit (0.7 mm diameter tip, Fine Science Tools, cat. no. 19008-07)
Guide cannula (BASi, cat. no. MD-2251)
Reference electrode: polyimide-insulated stainless steel electrode (0.01 in. diameter, 3 in. length, tapered tip size 8°, AC resistance 12 MΩ; A-M Systems, cat. no. 571500)
Flow injection system (University of Illinois at Chicago Research Resources Center, custom)

Polyimide-insulated stainless steel electrode (0.01 in. diameter, 3 in. length, tapered tip size 8°, AC resistance 12 MΩ; A-M Systems, cat. no. 571500)

Lesion-making device (Ugo Basile, cat. no. 53500)

Electric industrial heat gun (Weller, cat. no. 6966C)

Hardware:

- Multifunction input/output card: PCI-6052E (16 bit, 333 kHz) (National Instruments)
- Potentiostat: EI-400 biopotentiostat (Cypress Systems, cat. no. 66-El-400) or Custom (FSCV interface with integrated timing circuitry combined with amplifier/current-to-voltage converter headstage [Electronics and Materials Engineering (EME) Shop, Seattle, Washington]
- Headstage: low-pass-filtered amplifier/current-to-voltage headstage, standard amplification is 200 nA/V. Up to four channels for FSCV. Various configurations of this headstage allow for recording in small animals (mice, birds, fish) and larger animals such as rats and monkeys (EME Shop, Seattle, Washington; see Fig. 7.25.1B-C)
- Commutator: 9- or 25-channel (Crist Instruments, cat. no. 4-TBC-9 S or 4-TBC-25); a 25-channel commutator with a liquid tube cannula is also available from Crist Instruments for experiments that utilize a fluid line (cat. no. 4-TBC-9-LT) (Fig. 7.25.1B,C)
- Breakout box interface and power supply: a multifunction piece of equipment that separates digital and analog signals, sets the grounding scheme, reduces environmental noise, and filters and divides the applied waveform [custom; Electronics and Materials Engineering (EME) Shop, Seattle, Washington; Fig. 7.25.1A]
- Extra-tall behavioral chamber with TTL output card (DIG-726TTL) to allow for time-stamping animal- and machine-generated events in the voltammetry record (Med Associates, custom to accommodate experimental needs); the extra-tall chamber diminishes the probability of artifacts imparted to the recording because of the manipulator housing the electrode knocking into the roof or walls of the chamber (Fig. 7.25.1C)
- Computer with two, preferably three, full-height and full-length PCI slots

Hardware for stimulation:

- Digital-to-analog card: PCI-6711 (National Instruments, cat. no. 777740-01); this card is used in conjunction with the PCI-6052E (see Hardware, above) to reduce overlap of stimulation with the data acquisition scans
- Constant-current stimulator: e.g., Neurolog NL800 (Harvard Apparatus, cat. no. 650276), ISO-flex stimulus isolator (A.M.P.I., Jerusalem, Israel) or Model 2200 analog stimulus isolator (A-M Systems, cat. no. 850000) (Fig. 7.25.1A)

Software:

- Analysis software options include: HDCV (Bucher et al., 2013); TarHeel CV (UNC Electronics Facility); or Demon (Yorgason et al., 2011; Wake Forest Innovations) for: visualization of color plots and current traces; cutting and splicing voltammetry files to TTLs (recorded events); performing principal components analysis (chemometrics); and compiling chemometric data files for graphing and statistical analysis

Additional reagents and equipment for injection of rodents (*APPENDIX 4F*)

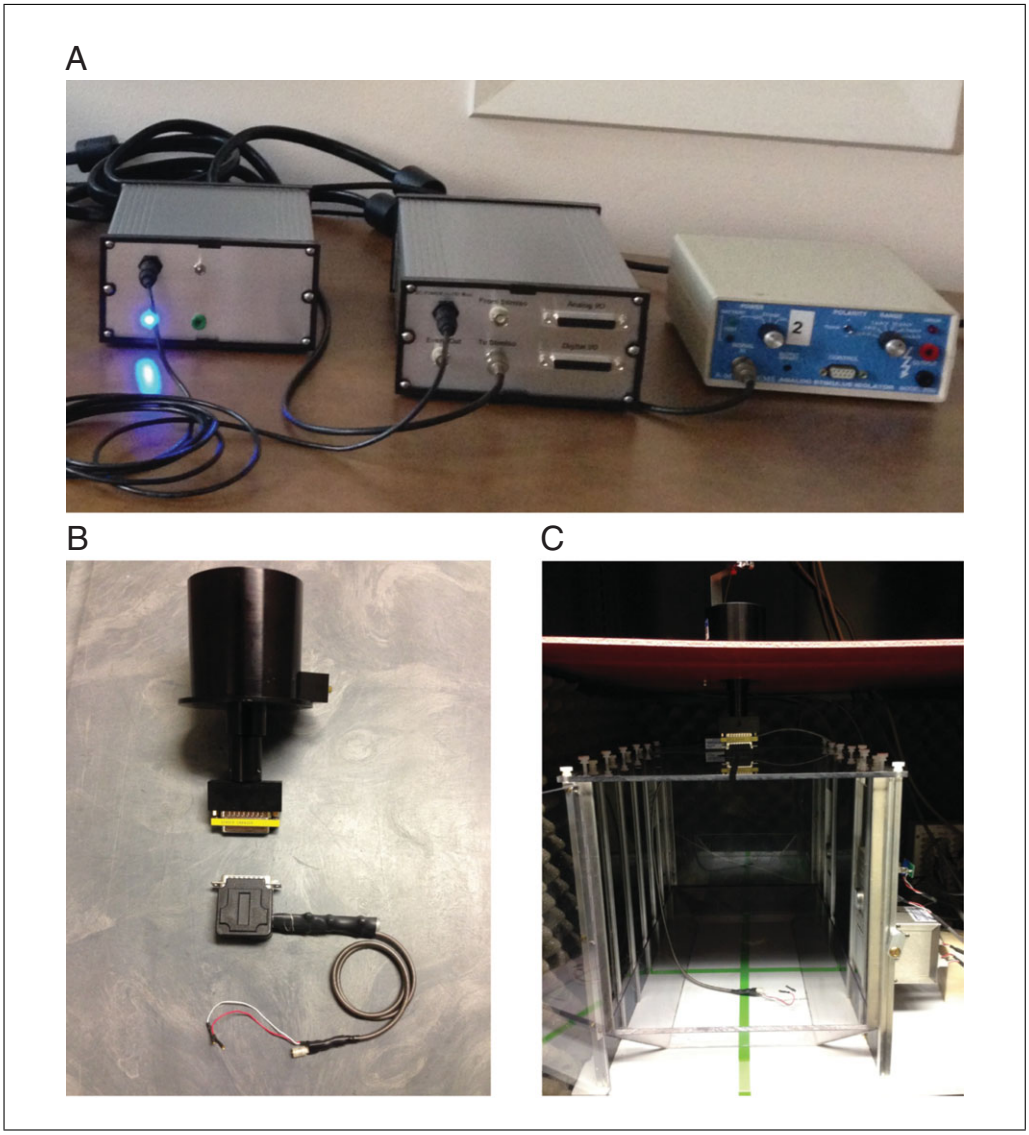

Figure 7.25.1 Necessary hardware for in vivo awake and behaving FSCV. (**A**) Breakout box interface (middle) with associated power supply (left) and Model 2200 analog stimulus isolator (right). (**B**) 25-channel commutator (above) and custom headstage (below). (**C**) Med-Associates behavioral chamber with commutator and headstage.

Fabricate a recording electrode for FSCV

Load glass with a single carbon fiber

1. Isolate a single carbon fiber, 7 μm in diameter and 10 cm long (length of the glass capillary), against the background of a well illuminated sheet of white paper taped to a flat surface. Tape one end of the fiber to the paper.

   It is important that a single fiber at least 10 cm long (length of glass capillary) be isolated.

2. Using a vaccum pump, aspirate the fiber through the 10-cm borosilicate glass capillary tube until the fiber extends from both ends.

3. Cut the fiber so it extends approximately 1 cm from each end of the glass tube.

Pull glass into two halves

4. Mark the midpoint of the capillary tube with a permanent marker.

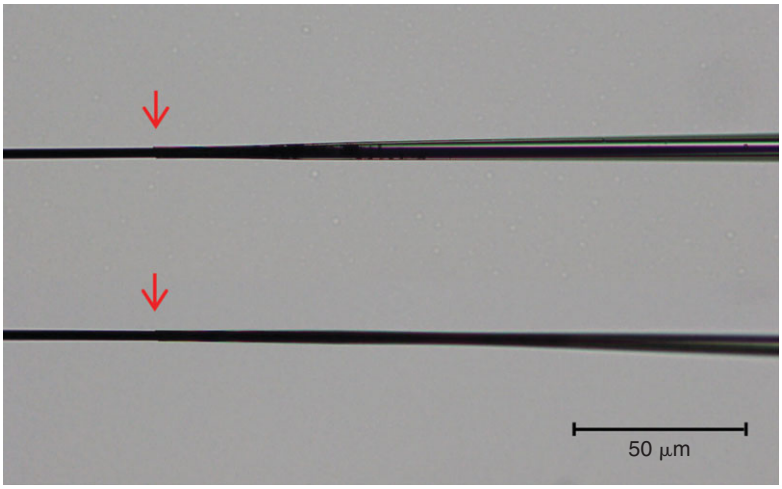

Figure 7.25.2 Carbon fiber recording electrodes with either a short, suboptimal taper (top) or long, ideal taper (bottom). Seals between the end of the glass pipet and protruding carbon fiber are indicated by red arrows. In our experience, the long, gradual taper and tight seal of the bottom electrode make it better suited for FSCV recordings of dopamine. 20× magnification.

5. Load the capillary tube into the vertical microelectrode puller with the marked midpoint positioned in the heating element of the puller.

   Precise positioning inside the heating element will depend on the desired length of the electrode. It is important to note that magnet and heat settings on the electrode puller will have to be optimized to achieve the correct-length taper ending in a tight glass seal around the carbon fiber (Fig. 7.25.2). Our experience has been that the best seals are made without the use of the magnet.

6. Pull the fiber-loaded capillary tube into two halves and cut the carbon fiber between the two halves with scissors before removing the electrodes from the puller.

   It is critical to note that not every electrode will be pulled with an acceptable seal. Care should be taken to visually inspect each seal before trimming and using electrodes.

Trim the carbon fiber

7. Use a scalpel with a #11 surgical blade to cut the carbon fiber extending through the tapered seal to 50 to 100 μm beyond the seal.

   To achieve the desired length, electrodes are cut under a light microscope using 10× magnification and a graticule in the eyepiece. To stabilize the electrode for cutting, the microscope slide is covered in clear packing tape and a small amount of sculpting putty is placed at the end of the slide to both stabilize and slightly angle the barrel end of the electrode. In addition to stabilizing the electrode for cutting, coating the microscope slide in packing tape helps to stabilize the scalpel during the cutting process. Only electrodes with a long, gradual taper to a tight seal around the carbon fiber should be cut (Fig. 7.25.2).

Make a connecting wire

8. Solder a small gold pin to the end of a 7.6-cm wire.

9. Slide the blue insulation of the wire along the wire until it is flush with the gold pin.

10. Cover the pin-wire connection with a 1-cm piece of 3 M heat shrinkable flexible polyolefin tubing (3/32 in. i.d.). Heat to shrink.

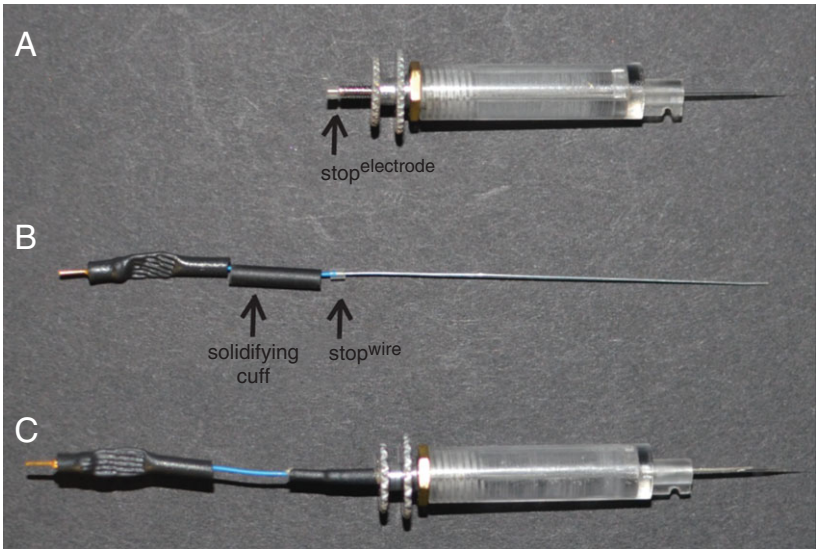

Figure 7.25.3 Construction of a manipulator-housed carbon fiber electrode. (**A**) A piece of capillary glass was loaded with a carbon fiber, pulled to form a taper and tight seal, and the fiber was cut to 50 to 100 μm before backloading through a micromanipulator. A 0.1-cm piece of heat-shrinkable tubing (stop^{electrode}) prevents the electrode from moving forward through the manipulator. (**B**) A constructed connecting wire with a 0.1-cm piece of heat-shrinkable tubing (stop^{wire}) and a 1-cm piece of heat-shrinkable tubing (solidifying cuff) in place. (**C**) A fully constructed microelectrode with solidifying cuff anchoring the wire to the manipulator.

11. Apply a 0.1-cm piece of heat-shrinkable tubing (3/64 in. i.d., clear) to the junction between the blue insulation and the bare wire to serve as a stop (stop^{wire}). Heat to shrink.

12. Thread a 1-cm piece of larger heat-shrinkable tubing (3/64 in. i.d.) up the wire, over the stop^{wire}, and to the end closest to the pin (Fig. 7.25.3). Do not heat to shrink.

    This piece of heat-shrinkable tubing serves to solidify the connection between the wire, glass capillary, and micromanipulator (solidifying cuff; as described in step 16).

Load a micromanipulator

13. Thread an electrode into the micromanipulator such that the non-tapered end of the electrode is inserted into the end of the micromanipulator that is opposite the screw stock. Secure the electrode in the manipulator with a 0.1-cm piece of heat-shrinkable tubing (3/4 in. id., clear) attached to the very back end of the glass capillary where it emerges from the screw stock of the manipulator (stop^{electrode}; Fig. 7.25.3A). Heat to shrink.

14. Coat the exposed portion of the connecting wire with a layer of Silverprint conductive paint and thread it through the lumen of the capillary until the stop^{wire} and stop^{electrode} pieces of heat-shrinkable tubing make contact.

    Take care to ensure that the wire is no longer than the length of the glass electrode before the taper, and cut if necessary.

15. Slightly rotate the wire while inserting it to ensure a connection between the wire and the carbon fiber.

16. Place the solidifying cuff over the stop^{wire}, stop^{electrode}, and 1 to 2 mm of the micromanipulator screwstock, and heat to solidify the assembly (Fig. 7.25.3).

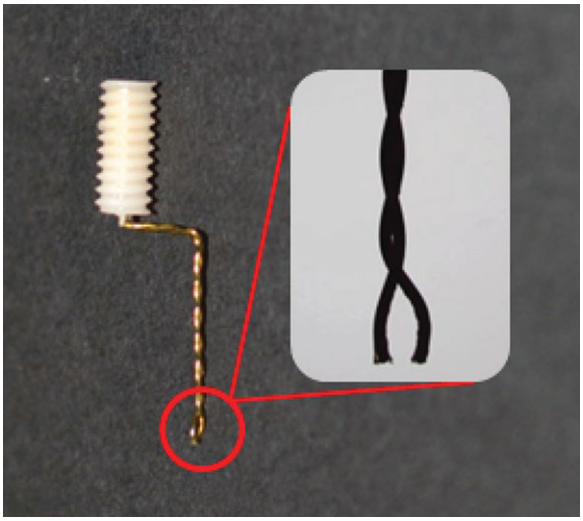

Figure 7.25.4 A shaped stimulating electrode. Note the 90° angle of the twisted stainless steel wires and the 1 mm terminal separation of the wires (1.25× magnification).

17. Clean the electrode tip by lowering it into purified and filtered isopropyl alcohol for 10 to 20 min before use.

18. Inspect the recording electrode before use under 10× magnification.

    It is important to confirm the integrity of the glass seal and the absence of cracks or other abnormalities, and that the carbon fiber makes contact with the wire in the lumen of the glass capillary tube.

Fabricate an Ag/AgCl reference electrode

19. Insert a 1-cm piece of silver wire (0.5 mm diameter) into the socket of a gold connector pin.

20. Apply a 5-min epoxy to the junction between the pin and the wire.

21. Chlorinate the silver reference electrode by electroplating in 1 N HCl.

    Reference electrodes should be chlorinated immediately before anesthetizing an animal for surgery. To chlorinate, connect the positive terminal of a 9 V battery to the gold pin of the reference electrode while the negative terminal is soldered to a wire (stainless steel or copper). Submerge both the negative terminal wire and silver wire of the reference electrode in 1 N HCl for approximately 30 sec. During plating, the acid surrounding the wire and the reference electrode should bubble and plating should be visible on the surface of the silver wire. Do not submerge the gold pin of the reference electrode. Allow the HCl to evaporate before implanting the reference electrode into the brain of the animal.

Shape a stimulating electrode

22. Bend stimulating electrode wires at a 90° angle from the base of the pedestal and again at a 90° angle about 5 mm down the wire from the first bend.

23. Separate the twisted wires of the stimulating electrode approximately 1 mm and cut them to equal lengths (Fig. 7.25.4).

Perform surgery

24. Anesthetize rat with intraperitoneal ketamine (100 mg/kg)/ xylazine (10 mg/kg).

    Intraperitoneal injection technique is described in APPENDIX 4F.

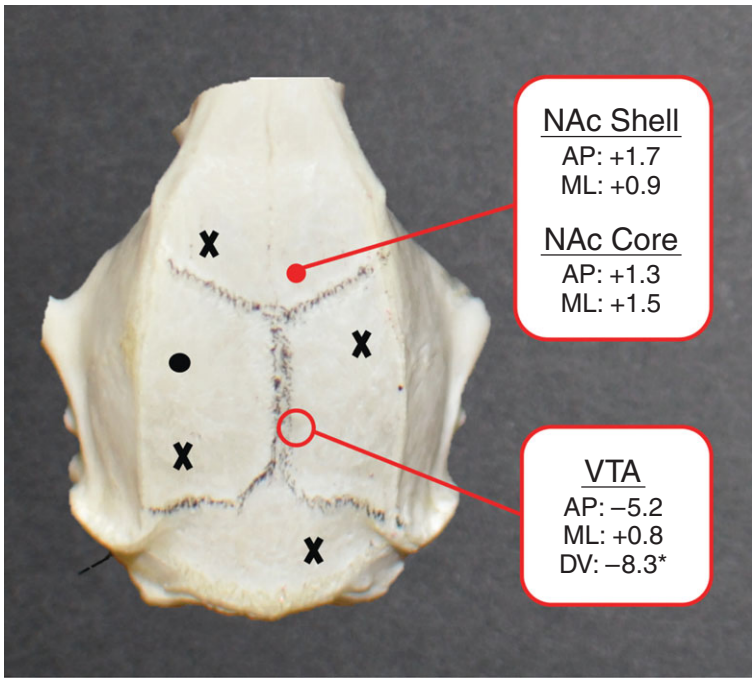

Figure 7.25.5 Dorsal surface of a rat skull with sutures emphasized for illustration of a surgical preparation. Closed circles indicate placement of drill holes for a reference electrode (black) and voltammetry cannula (red). The open red circle indicates placement of a larger hole for the stimulating electrode. Associated coordinates for a voltammetry cannula and stimulating electrode are listed (AP = anterior/posterior; ML = medial/lateral, relative to Bregma; DV = dorsal/ventral, relative to the brain surface). Refer to the section of the Basic Protocol describing surgically implanting animals for details regarding dorsal/ventral depth. *A* reference electrode hole is drilled on the skull over the contralateral forebrain. Four screws are secured in the locations indicated by a black X.

25. Shave the scalp and fix the head in a stereotaxic frame.
26. Clean the scalp with betadine and ethanol.
27. Make a 15-mm longitudinal incision along the midline of the scalp.
28. Clear underlying fascia with a scalpel and gauze.
29. Retract the skin to expose a 15-mm (longitudinal) × 10-mm (lateral) area of skull
30. Secure four stainless steel surgical screws (3/16 in.; Fig. 7.25.5) to the skull.
31. Drill holes over the desired targets [e.g., NAc for guide cannula; ventral tegmental area (VTA) for stimulating electrode] according to stereotaxic coordinates (Fig. 7.25.5).

    The hole for the stimulating electrode must be at least 1 mm in diameter to accommodate the electrode.

32. Lower a guide cannula, using the probe clamp stereotaxic frame attachment (see Materials list, above, as micromanipulators are designed to mate with this specific cannula; cut to 2.5 mm below the pedestal), over the dopamine terminal region of interest.
33. Place the reference electrode in the contralateral cortex.
34. Use dental acrylic to cement the reference electrode and guide cannula in place (Fig. 7.25.5).

If rats will be implanted with a stimulating electrode, care must be taken to avoid cementing over the drilled hole, the VTA, or the area behind it where the stimulating electrode pedestal will be placed.

35. If a stimulating electrode will be implanted, clear dura mater from the surface of the brain.

36. If applicable, lower the stimulating electrode and cement it in place.

    Prior to lowering, the stimulating electrode may need to be adjusted so that the stimulating prongs are straight in the anterior/posterior and medial/lateral planes. To optimize stimulating electrode placement, the stimulating electrode should first be lowered 7 mm into the brain. At this time, a recording electrode can be lowered through the guide cannula and to the level of the NAc, and FSCV performed while the VTA is stimulated (e.g., 150 μA, 4-msec monophasic current pulses; 60 pulses delivered at 60 Hz). FSCV software can be used in conjunction with stimulus isolators (e.g., Iso-Flex system from A.M.P.I., see Materials list, Hardware, above). The stimulating electrode should be lowered in 0.2-mm increments until robust dopamine release is detected at the recording electrode,and then cemented in place. In our experience, this depth is approximately 8.3 mm ventral to the brain surface. If a dopamine terminal region other than the NAc is being targeted, then the position of the stimulating electrode may need to be altered; for example, targeting the substantia nigra or medial forebrain bundle might be preferable.

Collect FSCV data from awake and behaving animals

Setup

37. Position the carbon electrode tip flush with the end of the micromanipulator and retract three complete clockwise turns such that the tip of the carbon fiber electrode is recessed into the lumen of the micromanipulator.

    This serves to protect the tip of the electrode during mating with the cannula and also helps track the depth of electrode as it courses through the brain. Each counter-clockwise full turn of the manipulator advances the electrode 0.33 mm.

38. Remove the BASi cannula obturator from the animal.

39. Tether the animal to the FSCV headstage via the implanted stimulating electrode and its corresponding cable that is part of the headstage assembly.

40. Insert the micromanipulator into the BASi cannula and lock it in place via a locking ring that is part of the guide cannula.

41. Connect both gold pins [mated to: (1) the Ag/AgCl reference electrode; and (2) the carbon fiber electrode] to their corresponding pins on the headstage.

42. Apply the "triangular" voltage waveform (referred to simply as triangular waveform; see "Set FSCV parameters," below) before power is delivered to the system.

Lower the carbon-fiber electrode

43. Lower the electrode into the brain region of interest.

    Targeting the NAc requires approximately 45 counter-clockwise turns of the manipulator (three turns to account for the recession of the electrode tip up the manipulator barrel, 25 turns to reach the bottom of the voltammetry guide cannula, and approximately 17 more turns to ultimately reach the NAc). The oscilloscope (part of the Tarheel CV software suite; see below) should be monitored for changes in background current with every manipulator turn, as a break in the electrode while lowering is evidenced by a sudden change in the shape or complete disappearance of the background. Usually, the background current will grow in size before collapsing when resistance is met in the brain that causes the glass to break (Fig. 7.25.6).

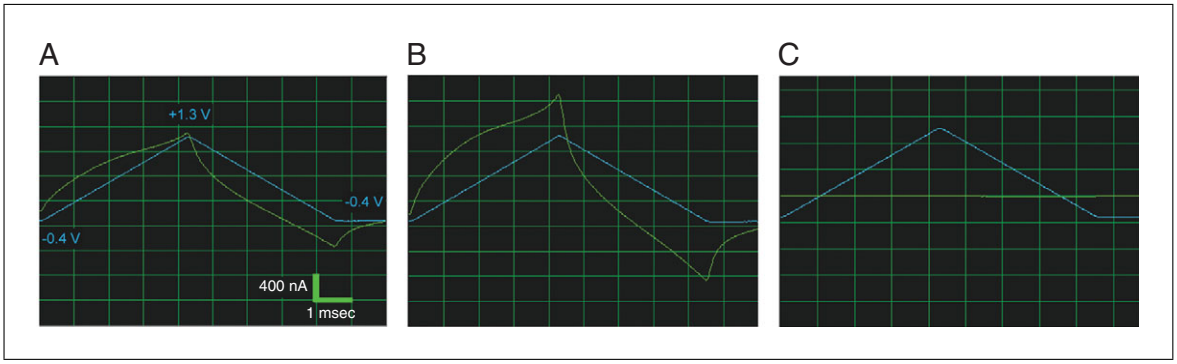

Figure 7.25.6 Background current produced by application of a triangular voltage waveform (blue line) as an electrode that breaks as it is lowered into the brain. (**A**) Background current (green trace) from a compromised electrode. Note the shape of the background current and the lack of an inflection in current during the anodic scan. (**B**) As this electrode was advanced through the brain, the background quickly increased before it was lost (**C**) due to a break of the carbon fiber at the level of the seal.

44. Secure the micromanipulator lock and allow the animal to move throughout the behavioral chamber.

    Typically, 30 min is allowed for behavioral habituation and electrode conditioning ("scanning"; see below).

Set FSCV parameters

45. To measure dopamine, hold the carbon fiber electrode at −0.4 V relative to the Ag/AgCl electrode. Set the software to change the voltage at a rate of 400 V/sec to +1.3 V and back to −0.4 V in a triangular waveform fashion (scan).

    Thus, the duration of each full scan is 8.5 msec.

Scan the electrode

46. Repeatedly apply the triangular waveform for 20 min at a rate of 60 Hz.

    Adequate scan time before beginning an experiment helps reduce background current drift that occurs with fresh carbon fiber electrodes. The rapid scan frequency increases the rate at which the electrode, and hence the background current, equilibrates to the local environment. As analysis for dopamine requires background subtraction, a stable background current is critical. Scan applications also etch the surface of the carbon fiber electrode to increase the adsorption of dopamine on the surface of the electrode (Heien et al., 2003). The electrode background should increase in size and take on a characteristic shape on the oscilloscope (Fig. 7.25.7).

47. Lower the frequency to 10 Hz for at least an additional 10 min before conducting experiments and recording at 10 Hz.

Apply stimulation

48. Set the frequency and duration of stimulation pulses using software (e.g., TarHeel CV).

49. Set the amplitude of current pulses using a stimulus isolator (e.g., ISO-Flex from A.M.P.I; see Hardware in the materials list, above).

    By implanting a stimulating electrode in the VTA, the delivery of current pulses to the dopamine cell bodies can act as a positive control for the detection of dopamine (Roitman et al., 2004) or can be used as a platform on which to examine the modulation of dopamine (Cone et al., 2013; Daberkow et al., 2013; Siciliano et al., 2014).

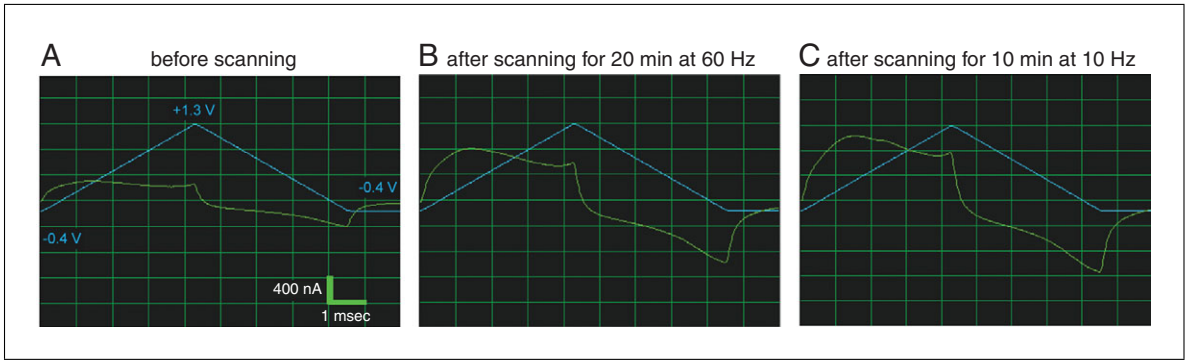

Figure 7.25.7 Background current produced by application of a triangular voltage waveform (blue line) as a carbon fiber electrode "scans" in the brain. Immediately after insertion into the brain, electrodes produce a background current (**A**) that gradually increases in size as the waveform is repeatedly applied (60 Hz) for 20 min. It should be noted that electrodes with good integrity normally display a background current where the time between the first peak on the anodic scan to the peak at the switching potential is 3 msec. (**B**) As the electrode equilibrates, the background potential increases. Switching the scanning frequency to 10 Hz (**C**) results in slight but stable changes in the shape of the background.

Synchronize FSCV with behavior

50. Turn on TTL pulses in FSCV software.

    Commercially available hardware and software for conducting behavioral experiments using animal subjects (e.g., MedAssociates) are designed to communicate with other systems using TTL pulses. FSCV software packages mentioned above capture TTL pulses, and thus dopamine concentration changes relative to discrete behavioral events can be analyzed.

Calibrate the FSCV recording electrode

51. Calibrate the FSCV recording electrode to assess the electrode's sensitivity to dopamine (see Sinkala et al., 2012, for details).

    Dopamine fluctuations are recorded in current (nA). To convert fluctuations in the dopamine-evoked current to dopamine concentration, each electrode should be calibrated in a known concentration of dopamine using a flow injection system. Sinkala et al. (2012) describe a flow injection system that is gravity fed and uses laminar flow to briefly expose an electrode to a known concentration of dopamine. Electrode sensitivity can vary as a function of brain tissue exposure (Logman et al., 2000) and length of exposed carbon fiber. While current as a function of concentration tends to be linear (Sinkala et al., 2012), for conservative calibrations, multiple concentrations of dopamine should be used.

Mark the carbon fiber placement

52. Backload a polyimide-insulated stainless steel electrode into a micromanipulator.

53. Advance the electrode to the same depth in the brain as the carbon fiber electrode during data collection.

54. Make an electrolytic lesion with a lesion-making device.

55. Remove the brain and process the tissue for the presence of a lesion using light microscopy.

    Slight differences in electrode placement in either the medial-lateral or dorsal-ventral planes can lead to the sampling of dopamine from functionally and/or histochemically different subterritories. As behaviorally relevant changes in dopamine concentration have been found to be regionally selective (Aragona et al., 2009; Brown et al., 2011; Wheeler et al., 2011; Willuhn et al., 2012), it is important to identify the recording location. One approach is to pass current through the carbon fiber to create a small lesion that can

be verified histologically (see Garris et al., 1994, or Park et al., 2009, for example). However, this destroys the electrode and does not allow an opportunity to calibrate the electrode after use. The alternative method is described above.

Data analysis

A variety of software programs are freely available for analysis of electrochemical data, including High Definition Cyclic Voltammetry (HDCV; University of North Carolina) and Demon Voltammetry and Analysis Software (Demon; Wake Forest University). Given that the use of HDCV and Demon are described in detail in previous publications [(Yorgason et al., 2011; Bucher et al., 2013, respectively], we will refrain from listing step-by-step instructions for analysis that depend on the specific software platform used by the experimenter.

Identifying dopamine release

Following background subtraction, changes in current over time at all applied scanning potentials are visually represented as a color plot (Fig. 7.25.9A). To determine if dopamine is present at a given time, current-by-voltage plots (background-subtracted cyclic voltammograms; CVs) can be constructed and examined. Figure 7.25.9 illustrates an example of stimulation applied to the dopamine cell bodies via a chronically implanted stimulating electrode. The current as a function of recording electrode voltage during the stimulation is plotted in Figure 7.25.9B. Prominent peaks at $\sim$ 0.6 V (0.645 V) on the anodic scan and ~ -0.2 V (-0.267 V) on the cathodic scan are indicative of dopamine. As the magnitude of oxidative current is directly proportional to dopamine concentration, the current at 0.645 V across time is plotted to determine the time course of changes in extracellular dopamine (Fig. 7.25.9C). Current changes are converted into concentration after data collection by calibrating the electrode in a flow injection system (see annotation to step 51, above) to determine the calibration factor (nA of current per nM of dopamine). This calibration factor can be used to calculate the concentration of a single dopamine release event or to statistically identify current changes that result from dopamine fluctuations (see "Chemometric analysis," below).

Chemometric analysis

The calibration factor along with example CVs (for example, obtained from electrical stimulation of the VTA) are used as inputs for chemometric analysis, which extracts dopamine concentration from the multivariate FSCV data obtained during awake and behaving experiments. Dopamine concentration can be extracted from electrochemical data using either principal component or partial least squares regressions (Heien et al., 2004; Faber and Rajkó, 2007; Hermans et al., 2008; Keithley et al., 2009, 2011). Both HDCV and Demon software have chemometric analysis features built in for extraction of dopamine concentration.

COMMENTARY

Background Information

FSCV involves the rapid application of a voltage ramp to an electrode which induces the oxidation and reduction of chemical species at the surface of the electrode that are electroactive within this voltage range. Electron transfer between the electrode surface and the analyte of interest is detected as current. Most studies using FSCV for the detection of dopamine make use of carbon fiber microelectrodes, although other surfaces and surface coatings have been used (Pihel et al., 1996; Singh et al., 2011; Tsai et al., 2012; Arumugam et al., 2013; Patel et al., 2013). The major advantage of FSCV, given that a range of voltages are applied to the electrode, is that these redox currents occur at unique potentials for each electrochemical species, thus allowing for multiple species to be detected and discriminated simultaneously (Heien et al., 2004; Keithley et al., 2009; Hashemi et al., 2011; Keithley and Wightman, 2011).

While other parameters have been used and ongoing work continues to focus on optimizing measurements (Keithley et al., 2011; Kile et al., 2012), here, and specifically for measuring dopamine in awake and behaving rodents, a nonoxidizing "holding potential" of −0.4 V, relative to an Ag/AgCl reference electrode, is applied to the carbon fiber. The potential is then ramped up to +1.3 V (anodic scan) and back down to −0.4 V (cathodic scan) at a rate of 400 V/sec. This triangular waveform of applied voltage can be repeated frequently. In practice, FSCV for dopamine detection in awake and behaving subjects employs a waveform application frequency of 10 Hz. Each application of the triangular waveform produces a large non-faradaic background current that is detected at the carbon fiber electrode. In addition, electrochemically active species will oxidize and reduce at known potentials along the scan. Dopamine oxidizes to dopamine ortho-quinone with the oxidation peak occurring at ∼0.65 V during the anodic scan and reduces from dopamine ortho-quinone back to dopamine with the peak reduction occurring at approximately −0.2 V during the cathodic scan.

When two electrons from the hydroxyl group of the catechol are shed and gained back, a faradaic current is produced which is added to the background current of the electrode at the potentials mentioned above. The stable background current on the electrode is typically 2 to 3 orders of magnitude greater than the current produced by dopamine detection. However, the background current is also stable from scan to scan and can therefore be subtracted out to leave only current *changes* over time. Using background subtraction, an increase in current at ∼0.65 V and a decrease at approximately −0.2 V is indicative of dopamine present at the electrode surface. Plotting current as a function of applied voltage generates a background-subtracted cyclic voltammogram (CV), which is used to identify an analyte, as the characteristic redox potentials are unique for different neurotransmitters and 'interfering' substances (e.g., changes in pH, ascorbic acid, and neurotransmitter metabolites; Smeets and González, 2000; Robinson et al., 2003; Heien et al., 2004). As the focus of this manuscript is on the detection of dopamine in behaving rodents, it should be noted that one confound is that CVs for dopamine and norepinephrine are indistinguishable. Thus, additional steps must be taken to dissociate changes in the two neurotransmitters if measurements are made in regions with substantial dopamine and norepinephrine inputs.

For a given release event, the current generated at the peak oxidation potential for dopamine is directly proportional to the concentration of dopamine at the sampling region of the electrode (Heien et al., 2004; Day et al., 2007; Anstrom et al., 2009; Jones et al., 2010). Analyzing the time course of current changes at the peak oxidation potential of dopamine can be used to understand the temporal dynamics of signaling during behavior or following experimenter-evoked release. The peak current resulting from a given release event is dependent on both the amount of dopamine released, as well as the sources that contribute to signal decay, such as reuptake by the dopamine transporter, diffusion, and breakdown by monoamine oxidase (MAO) or catechol-O-methyltransferase (COMT). The dynamics of dopamine release are easily visualized as a color plot, which displays current coded as color over time at all scanning potentials of the electrode (see Fig. 7.25.9 for example). Electrodes should be calibrated before or after use in vivo to convert current measured during an experiment into concentration of dopamine (Sinkala et al., 2012); however; some recent work suggests this conversion can be approximated from the magnitude of the electrode's non-faradaic background current (Roberts et al., 2013). Calibration is typically performed in a flow injection system where the electrode is bathed with buffer and a known concentration of dopamine (100 to 1000 nM) is briefly introduced. Following electrode calibration, principal component analysis (PCA) can be used to extract dopamine concentration from the electrochemical data (Heien et al., 2004; Keithley et al., 2009).

Critical Parameters and Troubleshooting

Surgery

The voltammetry cannula is lowered with the obturator (dummy stylet) in place. The cannula and the obturator fit together with a notch and are secured into place with an omega ring. It is critical that the notch and omega ring stay clear of dental cement during surgery, as separation of the obturator from the voltammetry cannula would otherwise be impossible. In addition, if cement were to obstruct part of the notch, the manipulator would not fully insert into the cannula and lock into place with the omega ring. In general, use caution when applying cement around the voltammetry cannula.

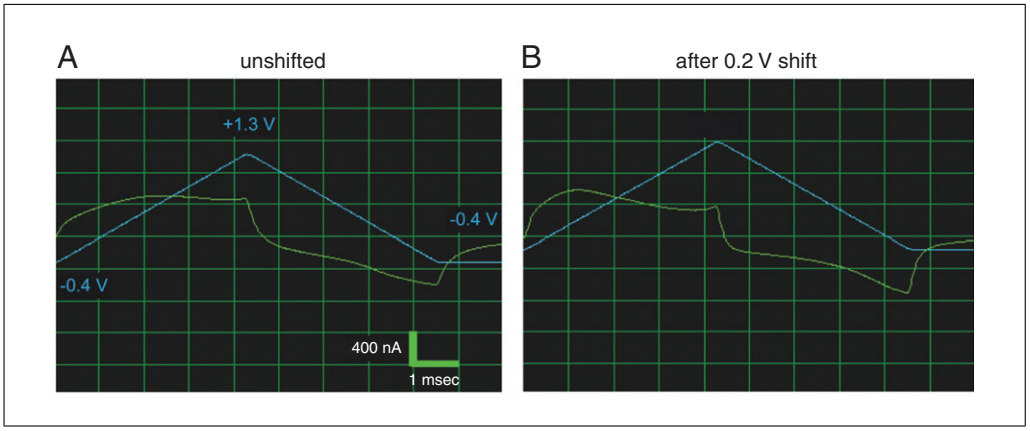

Figure 7.25.8 A "flattened" background current is observed if it is necessary to shift the applied voltage ramp. Electrode background currents that require shifting of the reference electrode have flattened background currents resulting from the anodic scan (**A**). Shifting the reference electrode by +0.2 V restores the characteristic shape of the anodic background current and increases the temporal difference between the peak of the background waveform and the point at which the background current crosses the applied waveform triangle (**B**).

Many experiments utilizing FSCV require a positive control to demonstrate detection of dopamine at the recording electrode. For this and other reasons, often a stimulating electrode is implanted at the site of the dopamine cell bodies. Twisted stainless-steel stimulating electrodes must be modified in order to maximize the space between the voltammetry cannula and the stimulating electrode. This is done so that the stimulator plug on the voltammetry headstage does not interfere with the ability to insert a manipulator into the voltammetry cannula.

FSCV in awake subjects requires multiple implants to be cemented together (headcap). Headcaps can be crowded, and for this reason, placement of headcap components should be planned ahead of surgery. The most common space constraint involves the stimulating electrode, as the headstage mount attaches to the stimulating electrode and is bulky. The stimulating electrode must therefore be constructed and oriented such that the mount is free from other cannulas when the stimulating electrode is in place. It is helpful to confirm adequate space and orientation before surgery begins. Confirm that the separated prongs of the stimulating electrode are straight in a medial/lateral plane and the 90° bend extends posteriorly. The headstage mount should plug in behind the site where the stimulating electrode is lowered into the brain. It is common to have to adjust the stimulating electrode in order to have the pedestal of the stimulating electrode in a position where it is free from other hardware. If the 90° bend of the stimulating electrode is anteriorly oriented (towards the voltammetry cannula), it can be impossible to plug a manipulator into the voltammetry cannula once the headstage is connected. If the manipulator and headstage touch, unnecessary mechanical noise will be introduced into the recordings. Screw placement is also critical; they must be placed such that they do not prohibit the lowering of the stimulating electrode to the appropriate depth or interfere with placement of the voltammetry cannula.

Electrode construction

Recording electrodes are hand made through a multistep process. It is imperative that electrodes be hand selected to meet criteria (outlined in the Basic Protocol), and that those not meeting the criteria be discarded. We estimate that only 30% of pulled electrodes are ever lowered into an animal, due to poor tapers, poor seals, wrong length of cut carbon fibers, poor electrical contact between the carbon fiber and connecting wire, or breakage during fabrication. At each step of construction, electrodes should be assessed for quality. Once an electrode is in the brain, its background current, as monitored on an oscilloscope, is the best way to quickly assess the quality of an electrode and to indicate those that are unlikely to yield good recordings and that should be replaced. If recordings are confounded with artifacts, oftentimes it is due to poor electrode quality. As it is common to have to switch electrodes, multiple electrodes should be prepared ahead of time for this purpose.

If an electrode breaks while in the animal's brain, the electrode should be raised and all

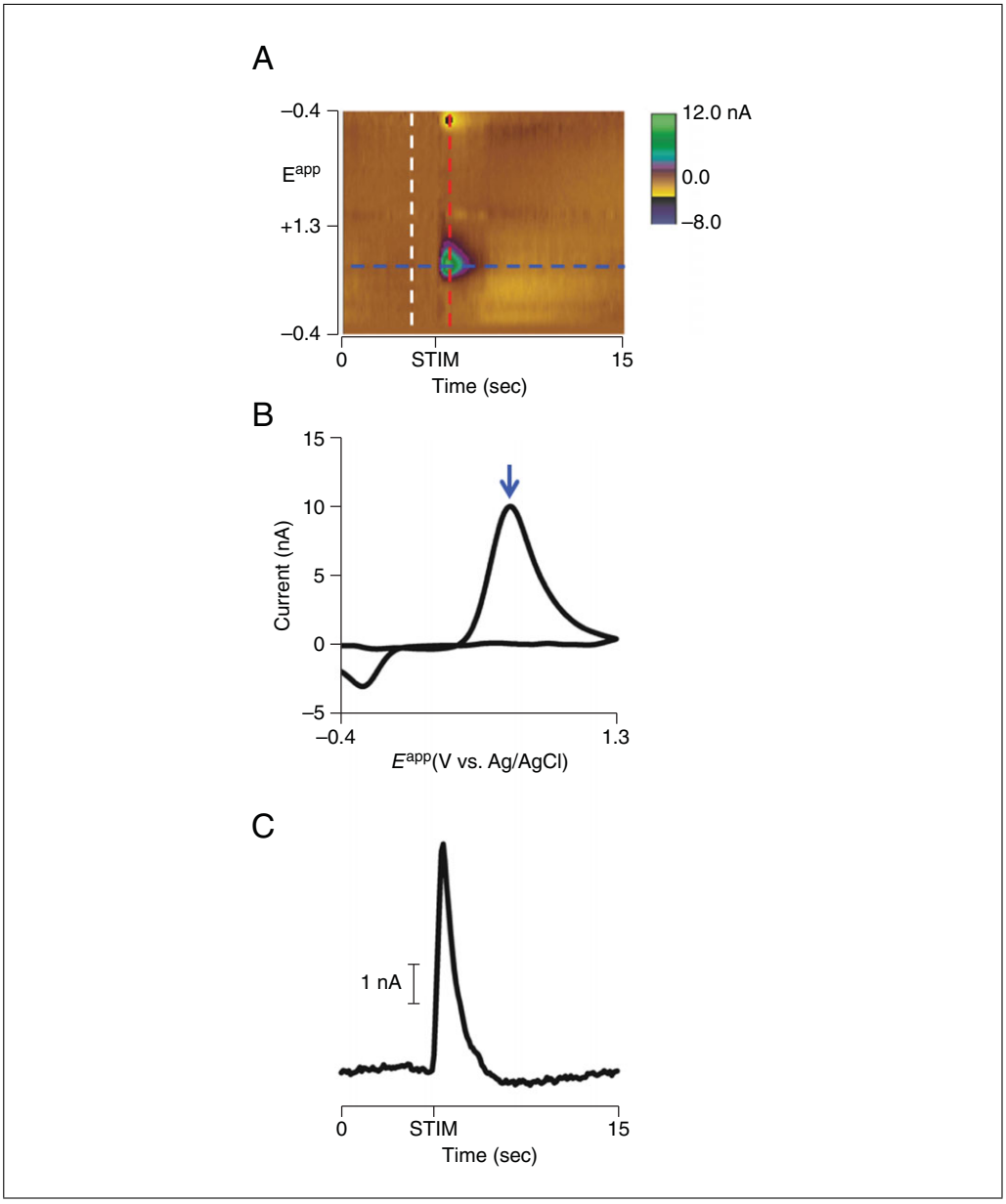

Figure 7.25.9 Visualization, confirmation, and quantification of currents resulting from an electrically stimulated dopamine release event (at "STIM"). (**A**) A background-subtracted color plot depicts changes in current (color) at a range of applied potentials (*y* axis) over time (*x* axis). As FSCV is a differential technique, background current, measured at approximately 1 sec before the time of the peak current (white dashed line), is subtracted from all applied potentials. To confirm that the current changes observed are from the oxidation and reduction of dopamine, a cyclic voltammogram (CV) (**B**) is generated by plotting the changes in background-subtracted current as a function of applied potential (red dashed line). The resulting CV is characteristic of dopamine, with a peak oxidation potential of 0.645 V (blue arrow in A and B). (**C**) To quantify the changes in dopamine resulting from electrical stimulation, current at the peak oxidation potential of dopamine is plotted over time (blue dashed line in A). In this example, electrical stimulation of the VTA evokes a 10.3-nA spike in current.

glass should be removed if possible. An obturator or lesioning electrode can be used clear the electrode path of any microscopic residual glass. Although the procedure is less likely to be successful, it is possible to lower a second electrode through the track of a broken one. Electrode breaks in vivo should rarely happen if electrodes are properly constructed and experiments occur within 10 days of surgery.

Shifting applied potential

Due to changes in the reference electrode that occur after extended time in the brain, it may be necessary to shift the applied

waveform by 0.2 V across all voltages. This situation is determined by monitoring the shape of the background current. On the anodic scan of an equilibrated electrode, there should be 3 msec between the first peak and the peak that occurs at the switching potential observed in the background current (Fig. 7.25.7B and C, for example). If there is less than 3 msec, as in Figure 7.25.8A, then the entire triangular waveform should be shifted by +0.2 V (−0.2 V to +1.5 V to −0.2 V; Fig. 7.25.8B).

Noise reduction

Mechanical and electrical noise are two frequently encountered issues during FSCV recordings. Attempts to reduce noise include the use of a Faraday cage, proper grounding techniques, use of shielded power cables, and insulation of pins and wires on the headstage. Headstage pins should be replaced regularly in order to ensure tight electrical connections between the headstage and electrode. Care should be taken to ensure that the wire and carbon fiber are sealed together with Silverprint paint in the barrel of the glass electrode before a recording begins. The micromanipulator lock should be checked to ensure tightness. As most noise arises from a compromised or subpar electrode, replacing it with a fresh one is a good initial troubleshooting step when encountering mechanical noise.

Anticipated Results

Dopamine will oxidize and reduce at characteristic potentials along the triangular waveform voltage scan (see Fig. 7.25.9 for example; ∼0.65 V for oxidation and ∼−0.27 V for reduction). Oxidation of dopamine can be verified using colorplots and CVs centered on the time point of interest. An example CV for dopamine is shown in Figure 7.25.9B. Note the large peak in current at 0.647 V. Monitoring this potential over time (blue arrow and blue dashed horizontal line in Fig. 7.25.9A), current evoked by stimulation of dopamine cell bodies can be seen to increase rapidly before decaying at an exponential rate (note that the decay is governed mostly by dopamine reuptake via the dopamine transporter). Dopamine release events also occur independently of electrical stimulation of the dopamine cell bodies. That is, they occur spontaneously or are evoked by behaviorally relevant stimuli. In general, these release events appear similar in shape and duration to electrically evoked dopamine release, but differ greatly in magnitude. Spontaneous or behaviorally evoked dopamine release events measure approximately 0.5 to 1.5 nA, while electrically evoked release via VTA stimulation with 120 μA (60 pulses at 60 Hz) can elicit anywhere from 1 to 50 nA (Fig. 7.25.9C). These figures can vary widely across animals, as the magnitude of release is dependent on numerous factors including placement of the stimulating electrode, number of release sites that the electrode is capable of detecting, and density of dopamine transporters in the vicinity of the electrode, as well as the characteristics of the recording electrode. Another important consideration is that kinetics of dopamine reuptake may differ across striatal subregions due to distribution of the dopamine transporter (Richfield, 1991; Ciliax et al., 1995; Wu et al., 2001; Brown et al., 2011). Decreases in current below baseline following dopamine release, especially after stimulated release, are most likely attributed to shifts in pH. A characteristic CV for a pH signal can be used to identify a pH shift (Takmakov et al., 2010), and chemometrics can be used to separate these signals from dopamine signals.

Time Considerations

Constructing the necessary electrodes (recording, reference and stimulating) to conduct an FSCV experiment in a cohort of four awake and behaving rats takes approximately 2 hr. Recording electrodes should be prepared in excess, as they often need to be replaced for various reasons (see Critical Parameters and Troubleshooting). Allot 6 hr to surgically implant a cohort of 4 rats. Less time will be needed if rats do not require a stimulating electrode. Data collection time varies with experiment and can take anywhere between 45 min and 4 hr for each rat. We estimate that data analysis, including electrode calibration, for each animal takes approximately 2 hr.

Acknowledgements

The authors acknowledge financial support from NIH Grant DA025634.

Literature Cited

Anstrom, K.K., Miczek, K.A., and Budygin, E.A. 2009. Increased phasic dopamine signaling in the mesolimbic pathway during social defeat in rats. *Neuroscience* 161:3-12.

Aragona, B.J., Day, J.J., Roitman, M.F., Cleaveland, N.A., Wightman, R.M., and Carelli, R.M. 2009. Regional specificity in the real-time development of phasic dopamine transmission patterns during acquisition of a cue-cocaine association in rats. *Eur. J. Neurosci.* 30:1889-1899.

Ariansen, J.L., Heien, M.L.A.V., Hermans, A., Phillips, P.E.M., Hernadi, I., Bermudez, M.A., Schultz, W., and Wightman, R.M. 2012.

Monitoring extracellular pH, oxygen, and dopamine during reward delivery in the striatum of primates. *Front. Behav. Neurosci.* 6:36.

Arumugam, P.U., Zeng, H., Siddiqui, S., Covey, D.P., Carlisle, J.A., and Garris, P.A. 2013. Characterization of ultrananocrystalline diamond microsensors for in vivo dopamine detection. *Appl. Phys. Lett.* 102:253107.

Baur, J.E., Kristensen, E.W., May, L.J., Wiedemann, D.J., and Wightman, R.M. 1988. Fast-scan voltammetry of biogenic amines. *Anal. Chem.* 60:1268-1272.

Brown, H.D., McCutcheon, J.E., Cone, J.J., Ragozzino, M.E., and Roitman, M.F. 2011. Primary food reward and reward-predictive stimuli evoke different patterns of phasic dopamine signaling throughout the striatum. *Eur. J. Neurosci.* 34:1997-2006.

Bucher, E.S., Brooks, K., Verber, M.D., Keithley, R.B., Owesson-White, C., Carroll, S., Takmakov, P., McKinney, C.J., and Wightman, R.M. 2013. Flexible software platform for fast-scan cyclic voltammetry data acquisition and analysis. *Anal. Chem.* 85:10344-10353.

Cheer, J.F., Aragona, B.J., Heien, M.L.A.V., Seipel, A.T., Carelli, R.M., and Wightman, R.M. 2007. Coordinated accumbal dopamine release and neural activity drive goal-directed behavior. *Neuron* 54:237-244.

Ciliax, B.J., Heilman, C., Demchyshyn, L.L., Pristupa, Z.B., Ince, E., Hersch, S.M., Niznik, H.B., and Levey, A.I. 1995. The dopamine transporter: Immunochemical characterization and localization in brain. *J. Neurosci.* 15:1714-1723.

Clark, J.J., Sandberg, S.G., Wanat, M.J., Gan, J.O., Horne, E.A., Hart, A.S., Akers, C.A., Parker, J.G., Willuhn, I., Martinez, V., Evans, S.B., Stella, N., and Phillips, P.E. 2010. Chronic microsensors for longitudinal, subsecond dopamine detection in behaving animals. *Nat. Methods* 7:126-129.

Cone, J.J., McCutcheon, J.E., and Roitman, M.F. 2014. Ghrelin acts as an interface between physiological state and phasic dopamine signaling. *J. Neurosci.* 34:4905-4913.

Cone, J.J., Chartoff, E.H., Potter, D.N., Ebner, S.R., and Roitman, M.F. 2013. Prolonged high fat diet reduces dopamine reuptake without altering DAT gene expression. *PLoS One* 8:e58251.

Daberkow, D.P., Brown, H.D., Bunner, K.D., Kraniotis, S.A., Doellman, M.A., Ragozzino, M.E., Garris, P.A., and Roitman, M.F. 2013. Amphetamine paradoxically augments exocytotic dopamine release and phasic dopamine signals. *J. Neurosci.* 33:452-463.

Day, J.J., Roitman, M.F., Wightman, R.M., and Carelli, R.M. 2007. Associative learning mediates dynamic shifts in dopamine signaling in the nucleus accumbens. *Nat. Neurosci.* 10:1020-1028.

Day, J.J., Jones, J.L., Wightman, R.M., and Carelli, R.M. 2010. Phasic nucleus accumbens dopamine release encodes effort- and delay-related costs. *Biol. Psychiatr.* 68:306-309.

Dreyer, J.K., Herrik, K.F., Berg, R.W., and Hounsgaard, J.D. 2010. Influence of phasic and tonic dopamine release on receptor activation. *J. Neurosci.* 30:14273-14283.

Ehrich, J.M., Phillips, P.E., and Chavkin, C. 2014. Kappa opioid receptor activation potentiates the cocaine-induced increase in evoked dopamine release recorded in vivo in the mouse nucleus accumbens. *Neuropsychopharmacology* doi: 10.1038/npp.2014.157.

Faber, N.M. and Rajkó, R. 2007. How to avoid over-fitting in multivariate calibration-the conventional validation approach and an alternative. *Anal. Chim. Acta* 595:98-106.

Flagel, S.B., Clark, J.J., Robinson, T.E., Mayo, L., Czuj, A., Willuhn, I., Akers, C.A., Clinton, S.M., Phillips, P.E.M., and Akil, H. 2011. A selective role for dopamine in stimulus-reward learning. *Nature* 469:53-57.

Garris, P.A., Ciolkowski, E.L., Pastore, P., and Wightman, R.M. 1994. Efflux of dopamine from the synaptic cleft in the nucleus accumbens of the rat brain. *J. Neurosci.* 14:6084-6093.

Garris, P.A., Christensen, J.R., Rebec, G.V., and Wightman, R.M. 1997. Real-time measurement of electrically evoked extracellular dopamine in the striatum of freely moving rats. *J. Neurochem.* 68:152-161.

Garris, P.A., Kilpatrick, M., Bunin, M.A., Michael, D., Walker, Q.D., and Wightman, R.M. 1999. Dissociation of dopamine release in the nucleus accumbens from intracranial self-stimulation. *Nature* 398:67-69.

Hashemi, P., Dankoski, E.C., Petrovic, J., Keithley, R.B., and Wightman, R.M. 2009. Voltammetric detection of 5-hydroxytryptamine release in the rat brain. *Anal. Chem.* 81:9462-9471.

Hashemi, P., Dankoski, E.C., Wood, K.M., Ambrose, R.E., and Wightman, R.M. 2011. In vivo electrochemical evidence for simultaneous 5-HT and histamine release in the rat substantia nigra pars reticulata following medial forebrain bundle stimulation. *J. Neurochem.* 118:749-759.

Heien, M.L.A.V., Johnson, M.A., and Wightman, R.M. 2004. Resolving neurotransmitters detected by fast-scan cyclic voltammetry. *Anal. Chem.* 76:5697-5704.

Heien, M.L.A.V., Phillips, P.E.M., Stuber, G.D., Seipel, A.T., and Wightman, R.M. 2003. Overoxidation of carbon-fiber microelectrodes enhances dopamine adsorption and increases sensitivity. *Analyst* 128:1413-1419.

Hermans, A., Keithley, R.B., Kita, J.M., Sombers, L.A., and Wightman, R.M. 2008. Dopamine detection with fast-scan cyclic voltammetry used with analog background subtraction. *Anal. Chem.* 80:4040-4048.

Iravani, M.M., Millar, J., and Kruk, Z.L. 1998. Differential release of dopamine by nitric oxide in subregions of rat caudate putamen slices. *J. Neurochem.* 71:1969-1977.

Jones, S.R., Lee, T.H., Wightman, R.M., and Ellinwood, E.H. 1996. Effects of intermittent and continuous cocaine administration on

dopamine release and uptake regulation in the striatum: In vitro voltammetric assessment. *Psychopharmacology* 126:331-338.

Jones, J.L., Day, J.J., Aragona, B.J., Wheeler, R.A., Wightman, R.M., and Carelli, R.M. 2010. Basolateral amygdala modulates terminal dopamine release in the nucleus accumbens and conditioned responding. *Biol. Psychiatr.* 67:737-744.

Keithley, R.B. and Wightman, R.M. 2011. Assessing principal component regression prediction of neurochemicals detected with fast-scan cyclic voltammetry. *ACS Chem. Neurosci.* 2:514-525.

Keithley, R.B., Heien, M.L., and Wightman, R.M. 2009. Multivariate concentration determination using principal component regression with residual analysis. *Trends Anal. Chem.* 28:1127-1136.

Keithley, R.B., Takmakov, P., Bucher, E.S., Belle, A.M., Owesson-White, C.A., Park, J., and Wightman, R.M. 2011. Higher sensitivity dopamine measurements with faster-scan cyclic voltammetry. *Anal. Chem.* 83:3563-3571.

Kile, B.M., Walsh, P.L., McElligott, Z.A., Bucher, E.S., Guillot, T.S., Salahpour, A., Caron, M.G., and Wightman, R.M. 2012. Optimizing the temporal resolution of fast-scan cyclic voltammetry. *ACS Chem. Neurosci.* 3:285-292.

Kishida, K.T., Sandberg, S.G., Lohrenz, T., Comair, Y.G., Sáez, I., Phillips, P.E.M., and Montague, P.R. 2011. Sub-second dopamine detection in human striatum. *PloS One* 6:e23291.

Kuhr, W.G. and Wightman, R.M. 1986. Real-time measurement of dopamine release in rat brain. *Brain Res.* 381:168-171.

Logman, M.J., Budygin, E.A., Gainetdinov, R.R., and Wightman, R.M. 2000. Quantitation of in vivo measurements with carbon fiber microelectrodes. *J. Neurosci. Methods* 95:95-102.

Natori, S., Yoshimi, K., Takahashi, T., Kagohashi, M., Oyama, G., Shimo, Y., Hattori, N., and Kitazawa, S. 2009. Subsecond reward-related dopamine release in the mouse dorsal striatum. *Neurosci. Res.* 63:267-272.

Owesson-White, C.A., Cheer, J.F., Beyene, M., Carelli, R.M., and Wightman, R.M. 2008. Dynamic changes in accumbens dopamine correlate with learning during intracranial self-stimulation. *Proc. Natl. Acad. Sci. U.S.A.* 105:11957-11962.

Owesson-White, C.A., Roitman, M.F., Sombers, L.A., Belle, A.M., Keithley, R.B., Peele, J.L., Carelli, R.M., and Wightman, R.M. 2012. Sources contributing to the average extracellular concentration of dopamine in the nucleus accumbens. *J. Neurochem.* 121:252-262.

Park, J., Kile, B.M., and Wightman, M.R. 2009. In vivo voltammetric monitoring of norepinephrine release in the rat ventral bed nucleus of the stria terminalis and anteroventral thalamic nucleus. *Eur. J. Neurosci.* 30:2121-2133.

Park, J., Takmakov, P., and Wightman, R.M. 2011. In vivo comparison of norepinephrine and dopamine release in rat brain by simultaneous measurements with fast-scan cyclic voltammetry. *J. Neurochem.* 119:932-944.

Parker, J.G., Zweifel, L.S., Clark, J.J., Evans, S.B., Phillips, P.E.M., and Palmiter, R.D. 2010. Absence of NMDA receptors in dopamine neurons attenuates dopamine release but not conditioned approach during Pavlovian conditioning. *Proc. Natl. Acad. Sci. U.S.A.* 107:13491-13496.

Patel, A.N., Tan, S., Miller, T.S., Macpherson, J.V., and Unwin, P.R. 2013. Comparison and reappraisal of carbon electrodes for the voltammetric detection of dopamine. *Anal. Chem.* 85:11755-11764.

Phillips, P.E.M., Robinson, D.L., Stuber, G.D., Carelli, R.M., and Wightman, R.M. 2003a. Real-time measurements of phasic changes in extracellular dopamine concentration in freely moving rats by fast-scan cyclic voltammetry. *Methods Mol. Med.* 79:443-464.

Phillips, P.E.M., Stuber, G.D., Heien, M.L.A.V., Wightman, R.M., and Carelli, R.M. 2003b. Subsecond dopamine release promotes cocaine seeking. *Nature* 422:614-618.

Pihel, K., Walker, Q.D., and Wightman, R.M. 1996. Overoxidized polypyrrole-coated carbon fiber microelectrodes for dopamine measurements with fast-scan cyclic voltammetry. *Anal. Chem.* 68:2084-2089.

Richfield, E.K. 1991. Quantitative autoradiography of the dopamine uptake complex in rat brain using [3H]GBR 12935: Binding characteristics. *Brain Res.* 540:1-13.

Roberts, J.G., Toups, J.V., Eyualem, E., McCarty, G.S., and Sombers, L.A. 2013. In situ electrode calibration strategy for voltammetric measurements in vivo. *Anal. Chem.* 85:11568-11575.

Robinson, D.L., Venton, B.J., Heien, M.L.A.V., and Wightman, R.M. 2003. Detecting subsecond dopamine release with fast-scan cyclic voltammetry in vivo. *Clin. Chem.* 49:1763-1773.

Roitman, M.F., Stuber, G.D., Phillips, P.E.M., Wightman, R.M., and Carelli, R.M. 2004. Dopamine operates as a subsecond modulator of food seeking. *J. Neurosci.* 24:1265-1271.

Runnels, P.L., Joseph, J.D., Logman, M.J., and Wightman, R.M. 1999. Effect of pH and surface functionalities on the cyclic voltammetric responses of carbon-fiber microelectrodes. *Anal. Chem.* 71:2782-2789.

Ryczko, D., Grätsch, S., Auclair, F., Dubé, C., Bergeron, S., Alpert, M.H., Cone, J.J., Roitman, M.F., Alford, S., and Dubuc, R. 2013. Forebrain dopamine neurons project down to a brainstem region controlling locomotion. *Proc. Natl. Acad. Sci. U.S.A.* 110:E3235-E3242.

Schluter, E.W., Mitz, A.R., Cheer, J.F., and Averbeck, B.B. 2014. Real-time dopamine measurement in awake monkeys. *PloS One* 9:e98692.

Schultz, W. 2013. Updating dopamine reward signals. *Curr. Opin. Neurobiol.* 23:229-238.

Siciliano, C.A., Calipari, E.S., Ferris, M.J., and Jones, S.R. 2014. Biphasic mechanisms of

amphetamine action at the dopamine terminal. *J. Neurosci.* 34:5575-5582.

Singh, Y.S., Sawarynski, L.E., Dabiri, P.D., Choi, W.R., and Andrews, A.M. 2011. Head-to-head comparisons of carbon fiber microelectrode coatings for sensitive and selective neurotransmitter detection by voltammetry. *Anal. Chem.* 83:6658-6666.

Sinkala, E., McCutcheon, J.E., Schuck, M.J., Schmidt, E., Roitman, M.F., and Eddington, D.T. 2012. Electrode calibration with a microfluidic flow cell for fast-scan cyclic voltammetry. *Lab Chip* 12:2403-2408.

Smeets, W.J.A.J. and González, A. 2000. Catecholamine systems in the brain of vertebrates: New perspectives through a comparative approach. *Brain Res. Rev.* 33:308-379.

Sossi, V. and Ruth, T.J. 2005. Micropet imaging: In vivo biochemistry in small animals. *J. Neural Transm.* 112:319-330.

Stamford, J.A. 1990. Fast cyclic voltammetry: Measuring transmitter release in "real time." *J. Neurosci. Methods* 34:67-72.

Stamford, J.A., Kruk, Z.L., Millar, J., and Wightman, R.M. 1984. Striatal dopamine uptake in the rat: In vivo analysis by fast cyclic voltammetry. *Neurosci. Lett.* 51:133-138.

Stuber, G.D., Klanker, M., de Ridder, B., Bowers, M.S., Joosten, R.N., Feenstra, M.G., and Bonci, A. 2008. Reward-predictive cues enhance excitatory synaptic strength onto midbrain dopamine neurons. *Science* 321:1690-1692.

Sugam, J.A., Day, J.J., Wightman, R.M., and Carelli, R.M. 2012. Phasic nucleus accumbens dopamine encodes risk-based decision-making behavior. *Biol. Psychiatr.* 71:199-205.

Swamy, B.E.K. and Venton, B.J. 2007. Subsecond detection of physiological adenosine concentrations using fast-scan cyclic voltammetry. *Anal. Chem.* 79:744-750.

Takmakov, P., Zachek, M.K., Keithley, R.B., Bucher, E.S., McCarty, G.S., and Wightman, R.M. 2010. Characterization of local pH changes in brain using fast-scan cyclic voltammetry with carbon microelectrodes. *Anal. Chem.* 82:9892-9900.

Tsai, H.-Y., Lin, Z.-H., and Chang, H.-T. 2012. Tellurium-nanowire-coated glassy carbon electrodes for selective and sensitive detection of dopamine. *Biosens. Bioelectron.* 35:479-483.

Venton, B.J., Troyer, K.P., and Wightman, R.M. 2002. Response times of carbon fiber microelectrodes to dynamic changes in catecholamine concentration. *Anal. Chem.* 74:539-546.

Venton, B.J., Michael, D.J., and Wightman, R.M. 2003. Correlation of local changes in extracellular oxygen and pH that accompany dopaminergic terminal activity in the rat caudate-putamen. *J. Neurochem.* 84:373-381.

Venton, B.J., Seipel, A.T., Phillips, P.E.M., Wetsel, W.C., Gitler, D., Greengard, P., Augustine, G.J., and Wightman, R.M. 2006. Cocaine increases dopamine release by mobilization of a synapsin-dependent reserve pool. *J. Neurosci.* 26:3206-3209.

Vickrey, T.L., Condron, B., and Venton, B.J. 2009. Detection of endogenous dopamine changes in *Drosophila melanogaster* using fast-scan cyclic voltammetry. *Anal. Chem.* 81:9306-9313.

Watson, C.J., Venton, B.J., and Kennedy, R.T. 2006. In vivo measurements of neurotransmitters by microdialysis sampling. *Anal. Chem.* 78:1391-1399.

Wheeler, R.A., Aragona, B.J., Fuhrmann, K.A., Jones, J.L., Day, J.J., Cacciapaglia, F., Wightman, R.M., and Carelli, R.M. 2011. Cocaine cues drive opposing context-dependent shifts in reward processing and emotional state. *Biol. Psychiatr.* 69:1067-1074.

Wightman, R.M., May, L.J., and Michael, A.C. 1988. Detection of dopamine dynamics in the brain. *Anal. Chem.* 60:769A-779A.

Willuhn, I., Burgeno, L.M., Everitt, B.J., and Phillips, P.E.M. 2012. Hierarchical recruitment of phasic dopamine signaling in the striatum during the progression of cocaine use. *Proc. Natl. Acad. Sci. U.S.A.* 109:20703-20708.

Wu, Q., Reith, M.E., Wightman, R.M., Kawagoe, K.T., and Garris, P.A. 2001. Determination of release and uptake parameters from electrically evoked dopamine dynamics measured by real-time voltammetry. *J. Neurosci. Methods* 112:119-133.

Yorgason, J.T., España, R.A., and Jones, S.R. 2011. Demon Voltammetry and Analysis software: Analysis of cocaine-induced alterations in dopamine signaling using multiple kinetic measures. *J. Neurosci. Methods* 202:158-164.